Prepared for the
National Institutes of Health
National Institute of Neurological Disorders and Stroke
Neural Prosthesis Program
Bethesda, MD 20892

ELECTRODES FOR FUNCTIONAL NEUROMUSCULAR STIMULATION

Contract #NO1-NS-32300

Quarterly Progress Report #6
1 December, 1994 - 28 February, 1995

Principal Investigator
J. Thomas Mortimer, Ph.D.

Co-Investigator
Warren M. Grill, Ph.D.

Applied Neural Control Laboratory
Department of Biomedical Engineering
Case Western Reserve University
Cleveland, OH 44106

Table of Contents

page

B. Electrode Design and Fabrication

B.2 Electrode Testing: Corrosion Testing of Cuff Electrodes 3

C. Assessment of Electrode Performance in an Animal Model
D. Modifications to Improve Functional Performance

C.2 Helical Spiral Cuff Electrodes 12

C/D Effects of Pulse Duration on Selectivity 13

Appendix I: Manuscript 14

Section B: Electrode Design and Fabrication

B.2 Electrode Testing: Corrosion Testing of Cuff Electrodes

Abstract

To investigate their resistance to corrosion, three 12-contact spiral cuff electrodes were stimulated continuously for 10 weeks while submerged in individual flasks containing phosphate buffered saline solution. Microscopic analysis of the contacts of the cuffs has begun. Evidence of defects in the contacts, unrelated to stimulation, has been found. Some stimulated related phenomena has been seen on contacts stimulated at the higher amplitudes. The evaluation of the contacts is continuing, as chemical analysis and examination of the welds is ongoing.

Previous Work

In previous progress reports (QPR #4 and #5), the experimental set-up and measurements made over the 10 week period were presented in detail. Briefly, three multiple contact spiral nerve cuff electrodes were immersed in individual flasks of saline solution and stimulated continuously for ten weeks. The contacts were stimulated with 1, 2, and 3 mA amplitude balanced charge rectangular pulses, with 50μs pulsewidth, at a frequency of 20Hz, and with a recharge limit of approximately 300μA. A schematic of the cuffs and the stimulation of each contact is presented in Figure 1.

After removing the cuffs from the flasks of saline, they were initially examined using a low power dissecting microscope. The contacts had a grainy, matte appearance that was not correlated with stimulation or stimulation amplitude.

To further investigate, initial SEM studies were performed on the contacts of one cuff, Cuff A. The contacts were removed from the silicone rubber cuff by cutting the silicone with a scalpel. Upon examination, adherent debris could be seen over much of the surface, obscuring surface detail and morphology. Scratches, scoring and pits could be seen, and were presented in the previous progress report. Additionally, figures were presented of the few welds that had been examined. In 2 of the 3 welds, only a few of the 7 strands of wire were incorporated in the weld.

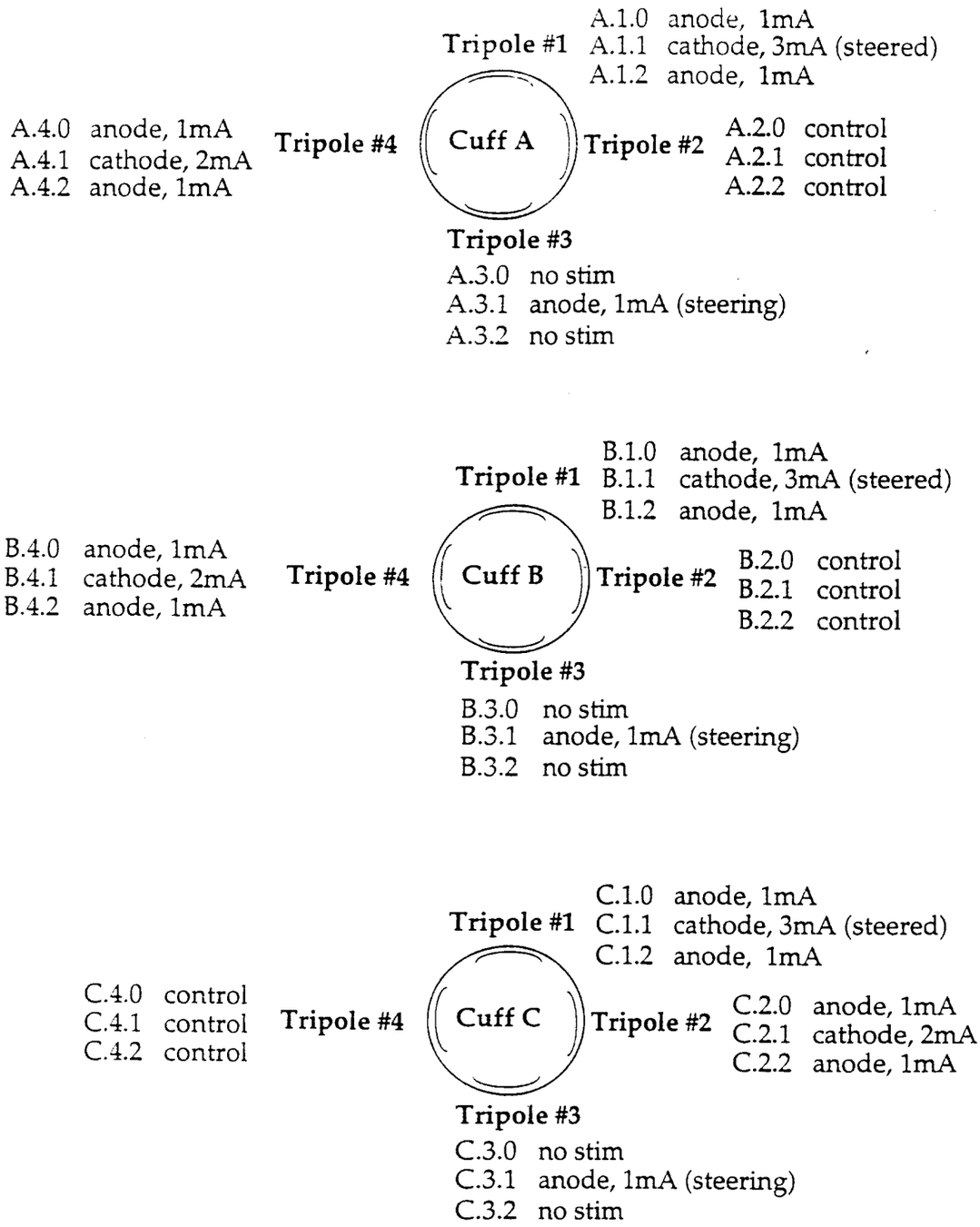

Figure 1: Cross-sectional schematic of the cuffs, with the stimulation and amplitudes of each contact indicated.

Continuing SEM Examination

For the remaining two cuffs, Cuffs B and C, attempts were made to improve the available surface detail by reducing the amount of surface debris seen in the SEM analysis of contacts from Cuff A. Prior to cutting the contacts out of the cuff, the intact cuff was first cleaned. This was performed with the cuff secured open using a locking forcep-type tool. The opened cuff was placed in a 1:100 solution of Liquinox in filtered water and sonicated for 10-15 minutes. The cuff was then rinsed 5 times with ultra-pure water, and again sonicated for 5 minutes in a fresh solution of ultra-pure water. The cuff was then soaked overnight in ethanol.

The contacts of the cuff were extracted from the silicone rubber sheeting by cutting the surrounding silicone with a scalpel blade. Efforts were made to keep a small length of wire attached to the contact, so as not to disturb the weld and to make it easier to handle the contact. After the contacts were extracted and labeled, they were individually cleaned under a Class 100 laminar flow hood. A contact (and the small length of attached wire) was sonicated first in a 1:100 solution of Liquinox in filtered water for 5 minutes, followed by a 1 minute sonication in ethanol. The contact was then placed on a clean room wiper, allowed to air dry, and was then placed on an SEM stage for future examination.

The cleaning regimen would appear to have been sufficient at removing much of the debris, as the contacts for Cuff B and Cuff C were much cleaner than those of Cuff A.

In the following four pages of figures (Figures 2-5), representative photomicrographs of the platinum contacts for each stimulation group (control, 1mA, 2mA, and 3mA) are presented. For the most part, these figures were taken from Cuffs B and C because the debris on contacts from Cuff A obscured much of the surface detail. Several phenomena were noted across these stimulation groups and are believed to be independent of stimulation. However, some features were seen only on those contacts stimulated at 2-3mA, indicating they are corrosion or stimulation related.

<u>Stimulation Independent Features</u>

Low power views (75-100x) of the platinum contacts are presented in the top portions of Figures 2-5 (2.a, 2.b, 3.a, 4.a, 4.b, 5.a and 5.b). Many score marks and gouging created by the tool used to cut the windows are evident in these figures and are consistent with what was reported in the previous progress report.

In many of these low power views, alterations in the surface appearance of the contacts, suspected of being related to the weld or the presence of the wires behind the contact can be seen. A slightly dimpled morphology and gross striations in the region over the weld and the wires was seen as compared to the rest of the contact. The dimpling is particularly evident in Figures 2.b and 2.d of control contacts, but was seen in contacts from other stimulation groups as well. The striations are presented in Figures 2.a and 3.d. This 'dimpling' may simply be a mechanical effect of the

wires being pressed against the contact, as occurs during the bonding of the silicone rubber sheets. Preliminary examination of these regions does not show any increased evidence of corrosion.

In half of the contacts from Cuffs B and C (12 of 24), tears or holes in the platinum foil were found. These defects were generally seen to be associated with the weld region and in most instances, extended from the edge of the contact inward. No correlation was found between these defects and the stimulation of the contact. Examples of these defects are presented in Figures 2.b, 2.c, 3.c, 4.b, 5.a, 5.b and 5.c. Again, a mechanical effect, stemming from two different mechanisms, may be primarily responsible for some of the tear defects. First, the contacts are pressed onto the wires during cuff manufacture. This could force the platinum to bend around the wire, being most severe at the edge of the contact. Second, the contacts, along with the rest of the cuff, are forced to bend inward due to the stretched silicone rubber sheet. This imposes some stresses onto the contact. Any loss of ductility, particularly with repeated opening and closing of the cuff, could lead to fracture of the metal.

Some of the defects appear to be strongly correlated to the welds themselves. Defects found in the weld regions of the contacts include holes, slits, and what may be burnthroughs, as shown in Figures 2.b, 2.c, 3.b, 4.b, and 4.c. Verification of this will be made through SEM examination of the backside of the contacts.

Several contacts exhibited lines of pits. These rows of pits were found over the entire surface of the contact, not just in that region that was exposed through the window in the silicone rubber sheeting. Examples of this are presented in Figures 2.d, 3.d and 4.d. The lines of pits were generally found to parallel the edge of the contact. This directional aspect of the pitting seems to implicate manufacturing processes that occurred in the production of the platinum foil. The contacts are cut from a larger piece of platinum foil and are generally square to one another. However, no specific information regarding the orientation of one contact to another or to the original sheet of platinum foil is recorded. Because these pits are found over the entire surface of the contacts, they do not seem to be related to corrosion phenomena, which would be expected only in the region of exposed metal. Additionally, this type of directional defect was seen in both control and stimulated contacts, and even on the backsides of some of the contacts that have been examined.

Stimulation Dependent Features

In those contacts that were stimulated at 2 and 3 mA, regions of a lighter color were seen in the exposed area of the contact. This is presented in Figures 3.a-3.d, 4.a, 4.b and 4.d. No chemical analysis has yet been performed to identify this apparent deposit. This lighter colored material was not seen on any of the unstimulated or 1 mA stimulated contacts. Additionally, it appears that more surface area on the 3mA stimulated contacts is covered with this deposit than is seen on the 2 mA stimulated contacts. Both of these

observations point to the deposit being a function of the stimulation and likely corrosion related.

Future Work

Several of the contacts have been examined only briefly, and a more thorough examination will be performed in the coming weeks. Additionally, the welds and backsides of the contacts for Cuffs B and C will be examined. Efforts will be made to determine the origin and nature of the apparent deposits seen on contacts that were stimulated at 2 and 3 mA. Compositional analysis may be performed in this regard.

Unstimulated Control Contacts

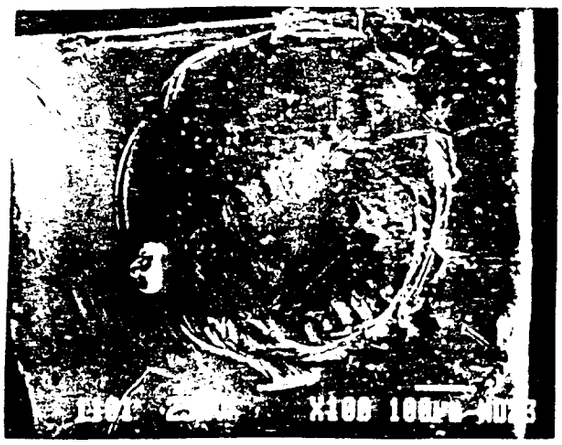

2.a: Photomicrograph of contact A.3.2

2.b: Photomicrograph of contact B.2.1

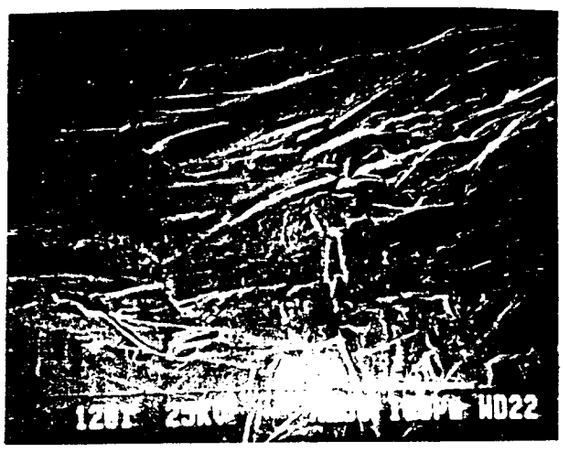

2.c: Photomicrograph of contact C.4.2

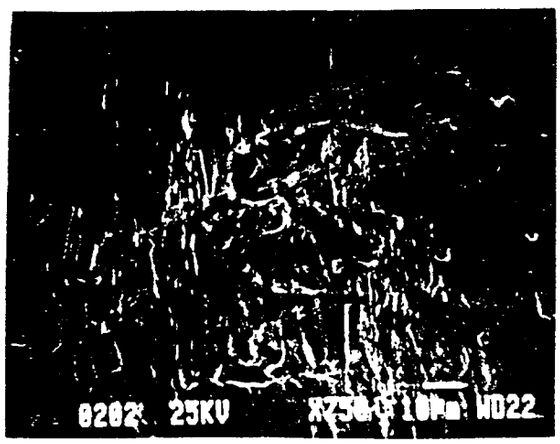

2.d: Photomicrograph of contact B.3.0

Figure 2: SEM photomicrographs representing unstimulated, control platinum contacts. Scoring and gouging are evident in 2.a and 2.b. Surface morphology differences, such as the striation-like marks in 2.a and the dimpling in 2.b and 2.d., were found in the areas overlying the welds and the wires. Tears are seen in 2.b and 2.c, a slit is seen in 2.c and directional lines of pits are seen in 2.d.

1mA Stimulated Contacts

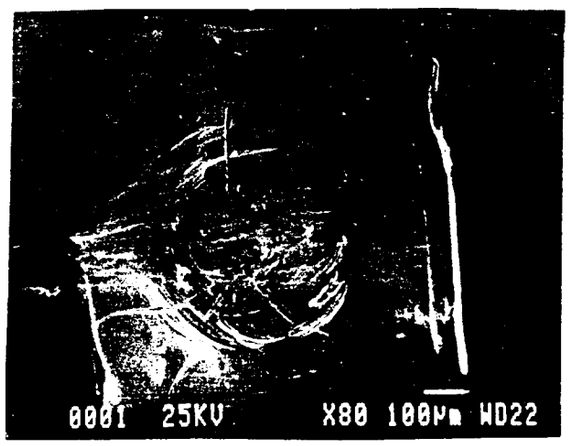

3.a: Photomicrograph of contact C.1.0

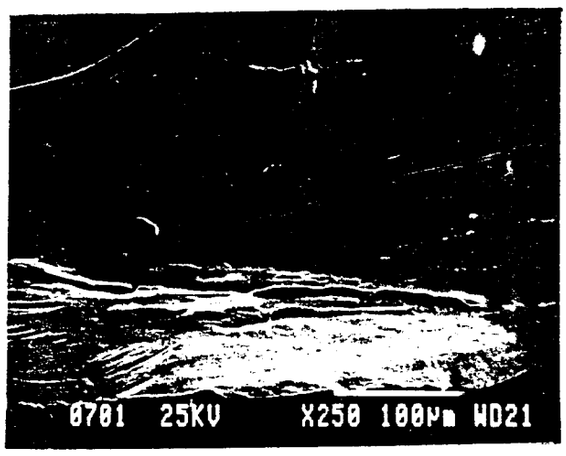

3.b: Photomicrograph of contact C.3.1

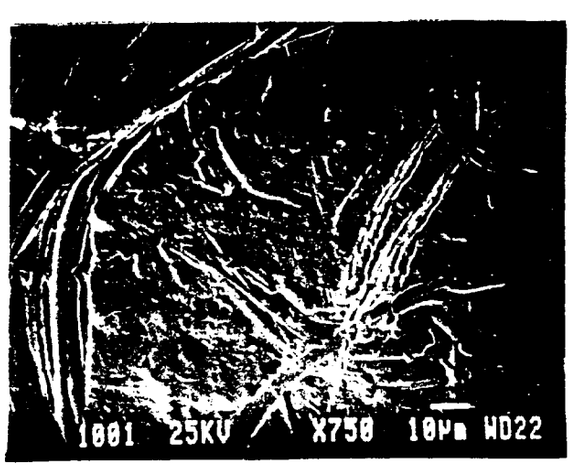

3.c: Photomicrograph of contact C.2.2

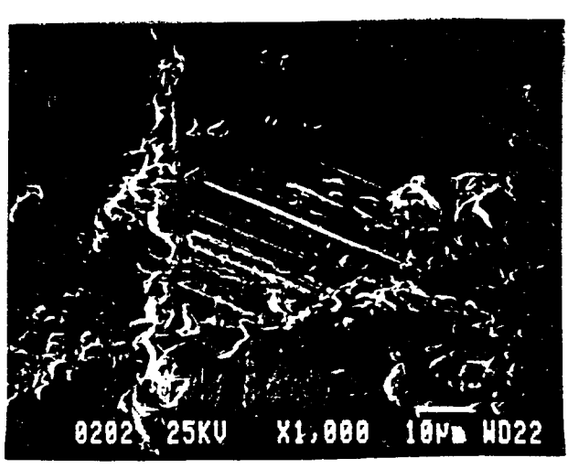

3.d: Photomicrograph of contact C.2.0

Figure 3: SEM photomicrographs representing 1mA stimulated platinum contacts. Scoring and gouging are evident in 3.a and 3.c. Surface morphology differences, such as the striation-like marks in 3.d and the dimpling in 3.a, were found in the areas overlying the welds and the wires. Tears are seen in 3.a and 3.b, a slit is seen in 3.b, and directional lines of pits are seen in 3.d.

2mA Stimulated Contacts

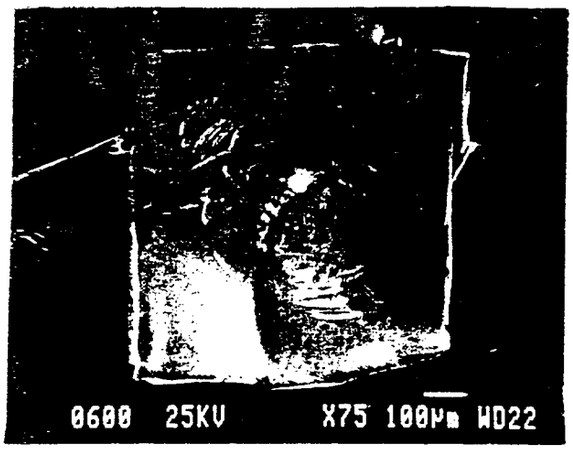

4.a: Photomicrograph of contact C.2.1

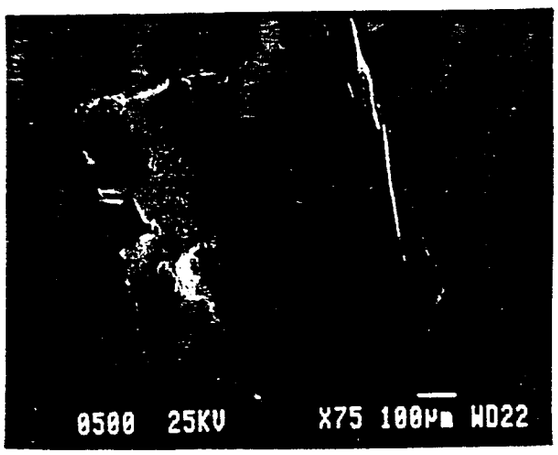

4.b: Photomicrograph of contact B.4.1

4.c: Photomicrograph of contact C.2.1

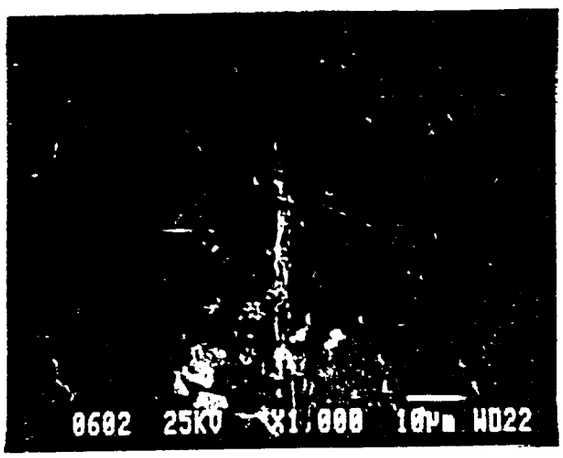

4.d: Photomicrograph of contact C.2.1

Figure 4: SEM photomicrographs representing 2mA stimulated platinum contacts. Scoring and gouging are evident in 4.a and 4.b. Surface morphology differences, such as the dimpling in 4.a and 4.b, were found in the areas overlying the welds and the wires. A tear is seen in 4.b as is a hole in the center, a possible burnthrough is presented in 4.c, and directional lines of pits are seen in 4.d. Light colored material appearing to be a deposit, can be seen in the exposed region of the contacts in all photos.

3mA Stimulated Contacts

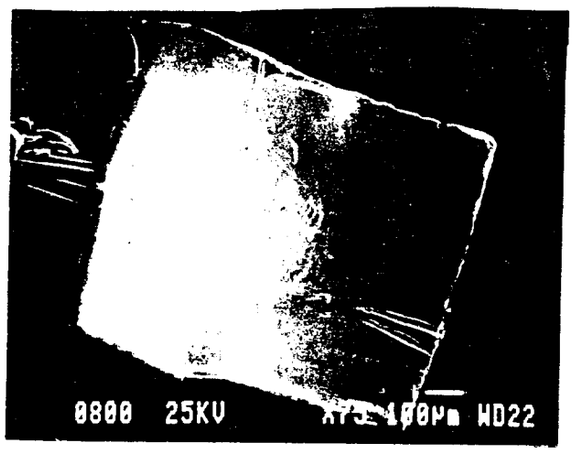

5.a: Photomicrograph of contact B.1.1

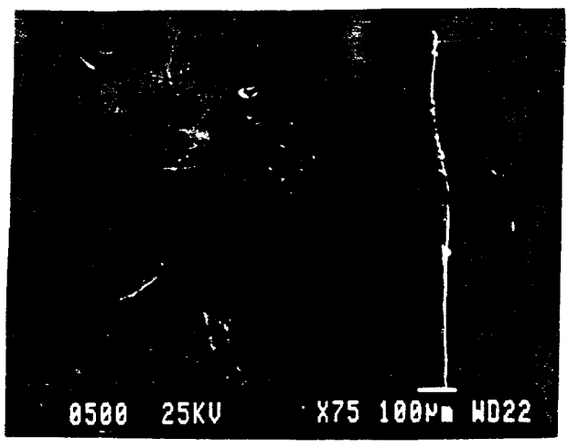

5.b: Photomicrograph of contact C.1.1

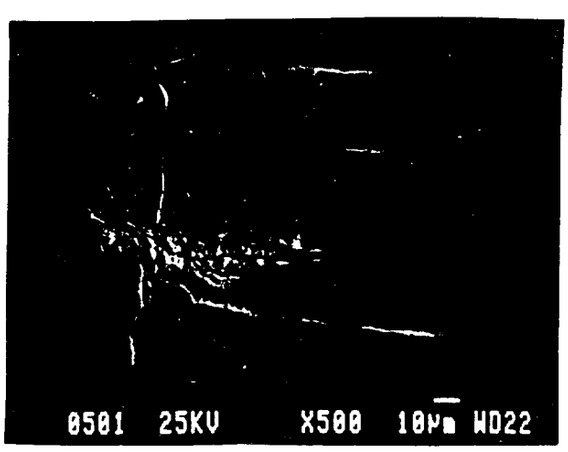

5.c: Photomicrograph of contact C.1.1

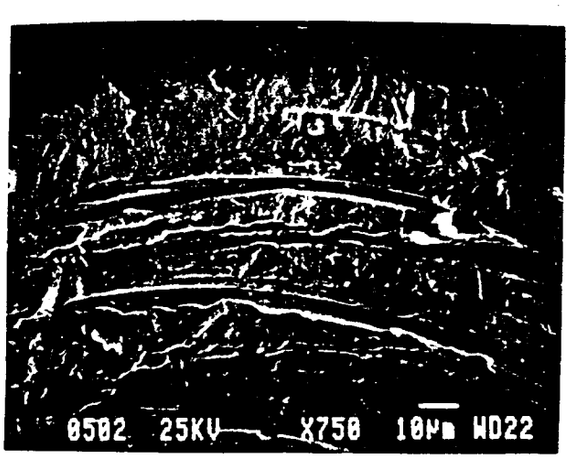

5.d: Photomicrograph of contact C.1.1

Figure 5: SEM photomicrographs representing 3mA stimulated (steered) platinum contacts. Scoring and gouging are evident in 5.a and 5.b. Surface morphology differences, such as the slight dimpling in 5.b, were found in the areas overlying the welds and the wires. Tears are seen in 5.a, 5.b and 5.c. Lighter colored material, appearing to be a deposit, was seen in the exposed region of the contacts, as shown in 5.a, 5.b and 5.d.

Section C: Quantitative Analysis of Electrode Performance in Acute and Chronic Animals

C.2 Helical-Spiral Nerve Cuff

Six helical-spiral nerve cuff electrodes were implanted on the left sciatic nerve of six animals for a 6-9 month period. One cuff had no wires while the other five had the wire back bone but no lead wire or stimulation contacts. During the implant, the helical spiral cuff was checked to verify that all wraps were properly positioned around the nerve. After the implant was completed, an x-ray of the hind limb was taken to record the implanted state of the cuff. At the end of the 9 month period another x-ray of the hind limb was made to record the final position of the cuff before explant. The animals were then perfused to fixate the tissue to check for any nerve damage. Explant of the cuff was then performed with care to not disturb the cuff's relative position to the surrounding tissue. Tissue samples of the nerve and the encapsulation were taken for histological studies. These samples are in the process of being prepared during the time of this writing.

From this experiment we discovered a problem. Of the six implants, in only one animal was the cuff found to be properly positioned around the nerve. In two of the animals, about one wrap was found to be positioned around the nerve while the remaining three were completely off the nerve. Of these three implants, one cuff was adjacent the nerve trunk and the other two cuffs were found in the subcutaneous space.

In order to investigate the possibility that the cuffs are coming off the nerve shortly after implant, three acute animals were implanted with similar helical-spiral cuffs and the hind limb was moved over the full range of motion. Periodic inspections of the cuff's position were performed with the hope of determining the cause for the cuff displacement. However, there was no occurrence of a cuff being displaced from the nerve.

We plan to continue this effort in another series of chronic experiments. In this series, x-rays will be performed at the time of implant, two, five, and ten days post-implant and then biweekly thereafter or until the cuff is found to have separated from the nerve. Through these efforts we hope to define the critical time when the electrode is most likely to be displaced from the nerve. From this we expect to determine the actual cause of the problem, propose a solution and make the appropriate modifications to the cuff's design or implant protocol to correct for these problems.

Section C: Quantitative Analysis of Electrode Performance in Acute and Chronic Animals
Section D: Modifications to Improve Functional Performance

C/D Effects of Pulse Duration on Selectivity

Computer simulations and chronic animal experiments have been performed to investigate the effect of pulsewidth on the selectivity of neural stimulation. It was found, both in the modeled behavior and in the animal tests, that shorter pulse duration allowed for improved selectivity. The studies performed and results obtained are described in the manuscript enclosed in Appendix I. This manuscript has been submitted to the journal *IEEE Transactions on Biomedical Engineering*.

Appendix I

The Effect of Stimulus Pulse Duration on Selectivity of Neural Stimulation

Warren M. Grill and J. Thomas Mortimer

submitted to
IEEE Transactions on Biomedical Engineering

THE EFFECT OF STIMULUS PULSE DURATION ON SELECTIVITY OF NEURAL STIMULATION

Warren M. Grill and J. Thomas Mortimer

wmg@po.cwru.edu
jtm3@po.cwru.edu

Applied Neural Control Laboratory
Department of Biomedical Engineering
Case Western Reserve University
C.B. Bolton Bldg., Rm. 3480
Cleveland OH 44106-4912 USA

ABSTRACT

Choice of stimulus parameters is an important consideration in design of neural prosthetic systems. The objective of this study was to determine the effect of rectangular stimulus pulsewidth (PW) on the selectivity of peripheral nerve stimulation. Computer simulations using a cable model of a mammalian myelinated nerve fiber indicated that shorter PWs increased the difference between the threshold currents of fibers lying at different distances from an electrode. Experimental measurements of joint torque generated by peripheral nerve stimulation demonstrated that shorter PWs generated larger torques before spillover and created a larger dynamic range of currents between threshold and spillover. Thus, shorter PWs allowed more spatially selective stimulation of nerve fibers. Analysis of the response of a passive cable model to different duration stimuli indicated that PW dependent contributions of distributed sources to membrane polarization accounted for the observed differences in selectivity.

INTRODUCTION

Electrical stimulation of the nervous system is a method to restore function to neurologically impaired individuals and a powerful tool to study the function of the nervous system. Stimulation of discrete populations of neurons is important to study the physiological effects of activation of different neural pathways, and is essential for efficacious multi-channel neuroprosthetics. Several electrode designs for spatially selective stimulation of peripheral nerve trunk regions are under development. Spatial selectivity is the ability to excite localized groups of nerve fibers in discrete fascicles or regions of fascicles within a nerve trunk. Peripheral nerve electrodes for selective stimulation include multiple contact nerve cuff electrodes [24], intrafascicular wire electrodes [27], intrafascicular silicon electrodes [19], wire electrodes sutured to the epineurium [22], and penetrating epineural electrodes [23]. All of these electrodes share the common goal of activating a discrete region of a peripheral nerve trunk. This has been accomplished by placing multiple, spatially distributed electrode contacts in or on different regions of a nerve trunk. Thus, proximity of the electrode to the nerve fibers targeted for activation has been the primary means to achieve selectivity.

In addition to electrode location, stimulus parameters may also affect the selectivity of neural stimulation. For example, short stimulus pulsewidths (PWs) increase the threshold difference between fibers with different diameters lying at the same distance from the electrode [5]. This allows the strength of contractions elicited by nerve stimulation to be graded [5, 11, 14], and may contribute to selective stimulation of muscles innervated by different diameter nerve fibers [21, 24]. Several investigators have attempted to define the volume of neural tissue stimulated by particular stimulus amplitudes [18]. However, they did not consider the possibility that stimulus parameters would affect selectivity.

The purpose of this study was to determine how stimulus PW affected the selectivity between nerve fibers at different distances from an electrode. This is an important consideration for selective stimulation of discrete groups of nerve fibers, regardless of electrode design. Computer simulations of the response of a mammalian myelinated peripheral nerve fiber were used to

determine the effect of stimulus PW on the threshold difference between fibers positioned at different distances from an electrode. Experimental measurements were then conducted to determine the effect of stimulus PW on selectivity between neighboring fascicles within the cat sciatic nerve. Finally, analysis of the response of a passive cable model to different duration stimuli was used to discern the underlying biophysical basis for the observed effects of stimulus PW. Preliminary results of this research have been published in abstract form [7].

METHODS

Computer Simulations

A computer model of a mammalian myelinated nerve fiber was used to predict the effects of stimulus pulsewidth (PW) on excitation. Myelinated nerve fibers were modeled using a 21 compartment cable model with the nodes of Ranvier described by mammalian non-linear membrane kinetics [20], and the myelin assumed to be a perfect insulator [10]. All model parameters and assumptions are the same as those of Warman et al. [25]. The first order non-linear differential equation describing the transmembrane voltage at each node was solved using the fourth-order Runge-Kutta method implemented in FORTRAN [20]. Criteria to recognize an action potential were transmembrane potential that exceeded 0 mV (rest potential was -80 mV) and a rate of change in transmembrane potential that exceeded 60 mV/ms. A simulation to determine the threshold current for one fiber configuration took approximately 2 min. on a Gateway 486/25. A passive cable model of a mammalian nerve fiber was used to examine the profiles of transmembrane polarization generated by different duration stimuli [25].

Experimental Procedures

Experiments were conducted in an animal model to determine the effects of stimulus PW on the selectivity of peripheral nerve stimulation. All animal care and experimental procedures were according to NIH guidelines and were approved by the Institutional Animal Care and Use Committee of Case Western Reserve University. Silicone rubber spiral nerve cuff electrodes,

containing 12 individually addressable platinum electrode contacts [24], were chronically implanted on the right sciatic nerve of 4 adult cats as part of a parallel study on the stability of nerve cuff recruitment properties. Measurements included in the present study were conducted at least 8 weeks after implantation of the electrodes.

For each testing session, animals were anesthetized with xylazine (Rompun, 2.0 mg/kg, SQ), masked with 3.0% gaseous Halothane in O_2, intubated, and maintained at a surgical level of anesthesia with 1.5-2.0% gaseous Halothane in O_2. A catheter was inserted in the cephalic vein and body temperature saline was administered (10 cc/kg/hour) during the testing interval (3-5 hours). Body temperature was maintained with a heating pad and heart and respiratory rates were continuously monitored.

Animals were mounted in a stereotaxic apparatus to measure the 3-dimensional isometric torque generated at the ankle joint by selective stimulation of the sciatic nerve [8]. Twitch contractions in the ankle musculature were generated using controlled current, biphasic, charge balanced, rectangular pulses applied at 0.5 Hz. Tripolar electrode configurations were used to localize the stimulation to discrete regions of the sciatic nerve trunk [21, 24]. The magnitude of the primary phase of the stimulus was stepped between 10μA and 2000μA to generate recruitment curves of torque as a function of stimulus current amplitude using different stimulus PWs (10μs-500μs). Stimulus amplitude was set manually with calibrated potentiometers while stimulus pulsewidth was controlled by the computer. The amplitude of the secondary phase of the stimulus was 100μA and its duration was imposed automatically by the stimulator to balance the charge delivered in the primary phase. The applied current was monitored on a storage oscilloscope by differentially measuring the voltage generated in a 100Ω resistor in series with the electrodes. Stimulus generation and response sampling were controlled using a multiple function input output board (NB-MIO-16H, National Instruments) in a Macintosh Quadra 950 and software written in LabVIEW (National Instruments). The ankle joint torque signals were low pass filtered at 100 Hz and sampled at 200 Hz with a 12-bit A/D converter. Five twitch responses were collected at each

stimulus amplitude and were averaged. The peak of the average torque twitch waveform was used as the measure of activation at each stimulus amplitude [8].

Analysis of Experimental Data

Recruitment curves of plantar-flexion/dorsi-flexion (PF/DF) torque as a function of the stimulus current amplitude were measured using each stimulus pulsewidth. Recruitment curves were parameterized by determining the threshold current amplitude, the current amplitude at spillover, the maximum torque before spillover, and the recruitment gain. Threshold was defined at the lowest current that generated at least 2N-cm of PF/DF torque. Spillover was defined as activation of a second fascicle and was determined by a sharp change in the slope of the recruitment curve (fig. 2A) and by a change in the direction of the joint torque vector in the PF/DF *vs.* external rotation/internal rotation plane [8].

Recruitment curves of joint torque as a function of the normalized stimulus amplitude were constructed by dividing the stimulus amplitudes by the threshold current amplitude at each pulsewidth. Dynamic range was determined from the normalized recruitment curves as the range of normalized stimulus amplitudes between threshold and spillover (fig. 2B).

The ability to grade contractions using different PW stimuli was determined by quantifying the recruitment gain over each recruitment curve. The torque values of each recruitment curve were normalized so the maximum torque was equal to 1, and current amplitudes were normalized so threshold was equal to 1. Normalized recruitment gain (NRG) was defined as the instantaneous slope of the normalized recruitment curve [6]. The mean NRG was then calculated over each recruitment curve from threshold to spillover. Statistical comparisons of experimental parameters were made using the non-parametric sign test [4].

RESULTS

Effect of Pulsewidth on the Current-Distance Relationship

The threshold current for activation of the model nerve fiber was dependent on the distance between the electrode and the nerve fiber, the nerve fiber diameter, and the stimulus pulsewidth (fig. 1). The threshold current at each pulsewidth (PW) was proportional to the square of the distance between the electrode and the nerve fiber ($r^2 \geq 0.969$). This is consistent with experimental measurements of the current-distance relationship for extracellular stimulation of axons [15]. The coefficient of proportionality, K, was a function of the stimulus PW, and the dependence could be described ($r^2 \geq 0.922$) using the Lapique equation given by (1).

$$K(PW) = \frac{K_{rh}}{1 - e^{-(PW/\tau)}} \qquad (1)$$

The time constant, t, was equal to 30.5 μsec, and the "rheobase" coefficient, K_{rh}, was equal to 1.1 mA/mm^2 for 10μm diameter fibers and 0.60 mA/mm^2 for 20μm diameter fibers. This compares well to previous estimates for K of 0.4-3 mA/mm^2 for activation of mediocaudal midbrain axons with 100μsec pulses [26] and 0.49-1.71 mA/mm^2 for activation of frog sciatic nerve fibers with 250μsec pulses [1]. Neither of these authors considered that K was a function of the stimulus PW.

The slope of the current-distance relationship was larger for shorter pulsewidths (fig. 1). The steeper current-distance curves indicated that shorter PWs generated larger differences between the threshold currents of fibers located at different distances from the electrode. The difference between the curves for different pulsewidths was greater when comparing pulsewidths that were less than the chronaxie [20]. Furthermore, the difference in slope at short and long pulsewidths was more pronounced as the distance between the electrode and the nerve fiber increased. These model results suggested that short PWs would provide more spatially selective activation of nerve fibers than long PWs.

Effect of Pulsewidth on Selectivity of Peripheral Nerve Stimulation

Recruitment curves of joint torque as a function of stimulus current amplitude were measured using four different stimulus PWs. The results of two separate experiments are shown in fig. 2. The tripolar electrode configurations used to generate these curves initially activated the innervation of the muscles producing dorsiflexion torques at the ankle joint (common peroneal fascicle innervating tibialis anterior and extensor digitorum longus). This was indicated by the negative torques in fig. 2. At higher stimulus current amplitudes, the activation spread to excite fascicles innervating the antagonist muscles that produced plantarflexion torques at the ankle (e.g., medial gastrocnemius, lateral gastrocnemius, soleus). Spillover to antagonist muscles appeared as an inflection in the recruitment curves (arrow in fig. 2A). As the stimulus amplitude was further increased, the net ankle joint torque moved in the positive or plantarflexion direction.

Shorter PWs increased the selectivity between different fascicles within the cat sciatic nerve. Two quantitative measures were used to quantify the selectivity achieved at different pulsewidths: the maximum torque generated before spillover and the dynamic range between the normalized current amplitude at spillover and the normalized current amplitude at threshold.

Short stimulus pulsewidths increased the maximum torque that could be generated before spillover. In the examples of figs. 2A and 2C this can be seen as the larger negative torques generated with the shorter pulsewidths before the inflection in the recruitment curves. This effect was consistent across experiments, and there were significant increases in the maximum torque generated before spillover with short pulsewidths compared with longer pulsewidths (Table 1). This effect was also progressive. As the stimulus pulse duration was reduced, the maximum torque generated before spillover increased, such that the largest differences occurred between the longest and shortest pulsewidths (Table 1).

Short pulsewidths also increased the dynamic range of currents between threshold and spillover, generating a larger region where the torque was a monotonically increasing function of the stimulus current amplitude. This can be seen in figs. 2B and 2D as the wider region between where the curve first deviates from zero (threshold) and the point of inflection in the recruitment

curves (spillover). The increase in dynamic range was consistent across experiments and there were significant increases in the dynamic range between all comparisons of shorter and longer pulsewidths. These results demonstrate that short PWs consistently generated more spatially selective activation than long PWs. As demonstrated in several previous studies, short pulsewidths also decreased the recruitment gain or slope of the recruitment curves (Table 1).

Biophysical Basis for Pulsewidth Dependent Selectivity

Extracellular stimulation generates a series of distributed sources along a nerve fiber, and the magnitude of these sources is equal to the spatial gradient of the extracellular field along the nerve fiber [10]. The primary determinant of polarization of a particular node of Ranvier is the gradient of the electric field outside that node (the "activating function") [16]. However, the activating functions at other nodes also affect the polarization of all other nodes along the fiber [25]. The contributions of the distributed sources (called the "ohmic" term) to the polarization of a particular node depends on the stimulus PW [25], and leads to pulsewidth dependent profiles of transmembrane polarization along nerve fibers. Figure 3 shows the profiles of transmembrane polarization (normalized to maximum depolarization), at the end of the stimulus pulse, generated by a 10μsec and a 100μsec stimulus pulse in two 10μm diameter nerve fibers positioned 0.5mm and 1.5mm from a point source electrode. The profiles of transmembrane polarization along the fibers vary with both the distance between the electrode and the fiber and the stimulus pulsewidth. The difference in polarization at the two pulsewidths is especially apparent at nodes 10 and 12 of the fiber positioned 0.5mm from the electrode. Similarly, these nodes are hyperpolarized in the close fiber, while they are depolarized in the more distant fiber.

Changes in transmembrane polarization, resulting from the pulsewidth dependent contributions of the ohmic term, account for the observed increases in selectivity at shorter pulsewidths. The effect of the ohmic term is to reduce the field gradient induced depolarization of fibers close to the electrode, and to increase the field gradient induced depolarization of fibers further from the electrode. This has the net effect, for a given stimulus amplitude, of bringing the

degree of depolarization in these two fibers closer together, and thus reducing the threshold difference between them.

The effect of the ohmic term on transmembrane polarization is summarized in fig. 4 for two different PWs. These data indicate that the ohmic contribution to membrane polarization caused a reduction in depolarization of the central node of nerve fibers close to the electrode (electrode to fiber distance <1.4 mm for 100μsec pulses and electrode to fiber distances <1.2mm for 10μsec pulses) and an increase in depolarization of the central node of fibers further from the electrode (electrode to fiber distance>1.4 mm for 100μsec pulses and electrode to fiber distances >1.2mm for 10μsec pulses). The net effect of the ohmic contribution to transmembrane polarization was to reduce the threshold difference between fibers at different distances from the electrode by reducing depolarization of the closest nerve fibers and increasing depolarization of more distant fibers. The steeper slope of the curve for 100μsec pulses confirms that the effect of the ohmic term on membrane polarization was greater for longer pulses. Short PWs minimize the effects of the ohmic term [25] and thus maintain the difference in depolarization between fibers at different distances from the electrode.

DISCUSSION

The results of this study demonstrate that the choice of stimulus pulsewidth affected the spatial selectivity of neural stimulation. Results from a cable model of a mammalian myelinated nerve fiber indicated that shorter PWs increased the slope of the current distance curve, and thus increased the threshold difference between fibers lying at different distances from the electrode. Experimental measurements of joint torque recruitment properties confirmed that shorter PWs provided greater selectivity between fascicles than did long PWs. Short PWs produced a significant increase in the maximum torque generated before spillover. This indicated that short PWs allowed activation of more fibers in a localized region of the nerve trunk before spillover occurred. Short PWs also produced a significant increase in the dynamic range between stimulus amplitude at threshold and stimulus amplitude at spillover. This indicated that short stimuli

reduced the spread of stimulation to adjacent fascicles. Similar observations were made in the central nervous system by Mihailovic and Delgado [13] who reported that

> *"In some cases increases in pulse durations increased the strength and the spread of the threshold response. In these cases the motor effects observed at threshold stimulation were more marked with pulse duration of 0.5 msec than with 0.01 or 0.1 msec. In other words, using pulses of longer duration at threshold stimulation a greater number of muscle units was simultaneously involved in the response than when shorter pulse durations were applied."*.

Examination of the profiles of transmembrane polarization in fibers at different locations using different PWs indicated that the contributions of sources present at other nodes along the fiber decreased the threshold difference between close and distant nerve fibers. The magnitude of the distributed sources is described by the activating function at each node of the fiber. Thus, the ohmic contributions depend on the profile of the activating function along the fiber, and therefore the electrode to fiber distance. The ohmic contribution to membrane polarization also depends on the stimulus duration. Short pulsewidths minimized the effects of ohmic sources on transmembrane polarization, and thus maintained the difference in polarization. The magnitude of the change in transmembrane polarization resulting from the ohmic contribution is equal to the difference between the activating function [16] and the total equivalent driving function [25].

Short PWs should be used for neural stimulation when maximal selectivity is desired because they improve the ability to activate discrete groups of nerve fibers. Short stimulus PWs also have additional characteristics that are beneficial to the performance of neural prostheses. First, short pulsewidths increase the threshold difference between different diameter nerve fibers [5]. This has the effect of reducing the slope of the recruitment curve and thus allowing electrically evoked muscle contractions to be more easily graded. This effect has been documented by several other investigators [5, 11, 14] and was also observed in this study (Table 1). More easily graded contractions (i.e., lower recruitment gain) will make robust control of electrically activated muscle easier. The results of the present study also suggest that some of the reduction in slope may have

been the result of increases in the threshold difference between fibers at different distances from the electrode in addition to the increases in threshold difference between different diameter nerve fibers. Short stimulus pulses also minimize the threshold charge (i.e., the amount of charge that must be injected to generated an action potential) [3]. Minimizing the injected charge is an important consideration for prevention of electrode corrosion which depends on the charge density on the electrode surface [17]. Short stimulus pulsewidths minimize the time available for irreversible electrochemical reactions to occur on the electrode [2]. These reactions can include oxygen reduction, which generates toxic oxygen radicals, hydrolysis of water, and electrode dissolution [12, 17]. Finally, short stimulus pulses may prevent stimulus induced neural damage [9].

ACKNOWLEDGMENTS

The authors thank Drs. D. Durand and P.H. Peckham for their comments on an earlier version of this manuscript, Ms. Nancy Caris and Ms. Jennifer Crossen for assistance during the animal experiments, Mr. Hani Kayyali for fabrication and maintenance of the laboratory stimulator, and Mr. Michael Miller for development of the data collection software. The software for the fiber model was obtained from Dr. D.H. Perkel and modified by Drs. J.D. Sweeney and E.N. Warman.

This work was supported in part by a grant from the Paralyzed Veterans of America and by NIH-NINDS Neural Prosthesis Program Contract N01-NS-3-2300.

REFERENCES

[1.] E.V. Bagshaw, M.H. Evans, Measurement of current spread from microelectrodes when stimulating within the nervous system. Exp. Brain Res. 25:391-400, 1976.

[2.] M.D. Bonner, M. Daroux, T. Crish, J.T. Mortimer, The pulse-clamp method for analyzing the electrochemistry of neural stimulating electrodes. J. Electrochemical Soc. 140:2740-2744, 1993.

[3.] P.E. Crago, P.H. Peckham, J.T. Mortimer, J.P. Van Der Meulen, The choice of pulse duration for chronic electrical stimulation via surface, nerve, and intramuscular electrodes. Ann. Biomed. Eng. 2:252-264, 1974.

[4.] I. Miller, J.E. Freund, R.A. Johnson, Probability and statistics for engineers. Prentice Hall, Englewood Cliffs, NJ, 1990, pp. 304-306.

[5.] P.H. Gorman, J.T. Mortimer, Effect of stimulus parameters on recruitment with direct nerve stimulation. IEEE Trans. Biomed. Eng. 30:407-414, 1986.

[6.] P.A. Grandjean, J.T. Mortimer Recruitment properties of monopolar and bipolar epimysial electrodes. Ann. Biomed. Eng. 14:53-66, 1983.

[7.] W.M. Grill, J.T. Mortimer, Non-invasive measurement of the input output properties of peripheral nerve stimulating electrodes, submitted to J. Neuroscience Methods, 1995.

[8.] W.M. Grill, J.T. Mortimer, Effect of stimulus pulsewidth on spatial selectivity of neural stimulation. Proc. 16th Ann. Int. Conf. IEEE-EMBS 16:363-364, 1994.

[9.] D.B. McCreery, W.F. Agnew, T.G.H. Yuen, L.A. Bullara, Damage in peripheral nerve from continuous electrical stimulation: comparison of two stimulus waveforms. Med. Biol. Eng. Comput. 30:109-114, 1992.

[10.] D.R. McNeal, Analysis of a model for excitation of myelinated nerve. IEEE Trans. Biomed. Eng. 23:329-337, 1976.

[11.] D.R. McNeal, L.L. Baker, J.T. Symons, Recruitment data for nerve cuff electrodes: implications for design of implantable stimulators. IEEE Trans. Biomed. Eng. 36:301-308, 1989.

[12.] S.L. Morton, M. Daroux, J.T. Mortimer, The role of oxygen reduction in electrical stimulation of neural tissue. J. Electrochemical Soc. 141:122-130, 1994.

[13.] L. Mihailovic, J.M.R. Delgado, Electrical stimulation of monkey brain with various frequencies and pulse durations. J. Neurophysiol. 19:21-36, 1956.

[14.] N. Nannini, K. Horch Muscle recruitment with intrafascicular electrodes. IEEE Trans. Biomed. Eng. 38:769-776, 1991.

[15.] J.B. Ranck, Jr., Which elements are excited in electrical stimulation of mammalian central nervous system: a review. Brain Res. 98:417-440, 1975.

[16.] F. Rattay, Analysis of model for extracellular stimulation. IEEE Trans. Biomed. Eng. 36:676-682, 1989.

[17.] L.S. Robblee, T.L. Rose, Electrochemical guidelines for selection of protocols and electrode materials for neural stimulation. in W.F. Agnew, D.B. McCreery, Eds., Neural Prostheses: Fundamental Studies, Prentice Hall, Englewood Cliffs, New Jersey, 1990, 25-66.

[18.] S.F. Ronner, Electrical excitation of CNS neurons. in W.F. Agnew, D.B. McCreery, Eds., Neural Prostheses: Fundamental Studies, Prentice Hall, Englewood Cliffs, New Jersey, 1990. 169-196.

[19.] W.L.C. Rutten, H.J. van Wier, J.H.M. Put, Sensitivity and selectivity of intraneural stimulation using a silicon electrode array, IEEE Trans. Biomed. Eng. 38:192-198, 1991.

[20.] J.D. Sweeney, D. Durand, J.T. Mortimer, Modeling of mammalian myelinated nerve for functional neuromuscular stimulation. Proc. 9th Ann. Int. Conf. IEEE-EMBS, 1577-1578, 1987.

[21.] J.D. Sweeney, D.A. Ksienski, J.T. Mortimer, A nerve cuff technique for selective excitation of peripheral nerve trunk regions. IEEE Trans. Biomed. Eng. 37:706-715, 1990.

[22.] H. Thoma, W. Girsch, J. Holle, W. Mayr Technology and long-term application of an epineural electrode. Trans. Am. Soc. Artif. Int. Organs 35:490-494, 1989.

[23.] D.J. Tyler, D.M. Durand, Design and acute test of a radially penetrating interfascicular nerve electrode. Proc. 15th Int. Conf. IEEE-EMBS 15(3):1247-1248, 1993.

[24.] C. Veraart, W.M. Grill, J.T. Mortimer, Selective control of muscle activation with a multipolar nerve cuff electrode. IEEE Trans. Biomed. Eng. 40:640-653, 1993.

[25.] E.N. Warman, W.M. Grill, and D. Durand, Modeling the effects of electric fields on nerve fibers: determining excitation thresholds. IEEE Trans. Biomed. Eng. 39:1244-1254, 1992.

[26.] J. Yeomans, P.Prior, F. Bateman, Current-distance relations of axons mediating circling elicited by midbrain stimulation. Brain Res. 372:95-106, 1986.

[27.] K. Yoshida, K. Horch, Selective stimulation of peripheral nerve fibers using dual intrafascicular electrodes. IEEE Trans. Biomed. Eng. 40:492-494, 1993.

FIGURE LEGENDS

Figure 1: Threshold current to excite a 10μm myelinated nerve fiber as a function of the electrode to fiber distance using four different rectangular stimulus pulsewidths. The model nerve fiber was positioned in a homogeneous, isotropic medium adjacent to a monopolar point source stimulating electrode. The slope of the current-distance curve increased as the pulsewidth was decreased, indicating that short stimulus pulsewidths increased the threshold difference between fibers at different distances from the electrode.

Figure 2: Experimental measurements of the effect of stimulus pulsewidth on selective neural stimulation with a multiple contact cuff electrode. A, C. Recruitment curves of plantar-flexion/dorsi-flexion (PF/DF) torque as a function of the stimulus current amplitude using four different stimulus pulsewidths. In both cases, shorter pulsewidths increased the maximum dorsiflexion torque that could be generated before spillover to antagonist muscles. B, D. Recruitment curves of PF/DF torque as a function of the normalized stimulus current amplitude. In both cases shorter pulsewidths increased the dynamic range of stimulus current amplitudes between threshold and spillover.

Figure 3: Profiles of transmembrane polarization between nodes 4 and 18 of two 10μm nerve fibers positioned either 0.5 mm or 1.5 mm from a point source stimulating electrode. The profiles were calculated using the total equivalent driving function [25], and normalized by dividing by the maximum depolarization generated in each case. The profiles vary with the distance from the electrode (due to changes in the activating functions along the fiber) [16], and with the stimulus pulsewidth (due to pulsewidth dependent contributions of the ohmic term to membrane polarization) [25].

Figure 4: Changes in transmembrane polarization that resulted from the contributions of the ohmic term. Curves are plotted for two different stimulus pulsewidths as a function of the distance between a point source electrode and a 10μm nerve fiber. Changes in polarization were calculated

for the central node of the fiber by taking the difference between the actual membrane polarization (the total equivalent driving function [25]) and the membrane polarization predicted by the activating function [16], which neglects the contribution of the ohmic term expressed as a percentage of the actual transmembrane polarization. The ohmic contribution reduced the difference between the amount of depolarization generated in near and distant nerve fibers. This effect was dependent on stimulus pulsewidth such that short stimulus pulsewidths maintained to a greater degree the threshold difference.

Table 1: Effects of Stimulus Pulsewidth on Recruitment Parameters.

The table values indicate the mean difference between the parameters for each of the two pulsewidths given in the left column (parameter at shorter pulsewidth-parameter at longer pulsewidth). The p-values are the results of a sign-test to reject the hypothesis that the parameters were the same for the two pulsewidths.

		Dynamic Range		Maximum Torque		Recruitment Gain	
PW	n	Mean Difference (% of threshold)	p≤	Mean Difference (N-cm)	p≤	Mean Difference	p≤
10-50	7	0.57	0.004	3.6	0.008	-1.2	0.031
10-100	7	0.67	0.004	4.4	0.004	-1.9	0.031
10-500	17	0.56	0.001	7.4	0.001	-0.7	0.029
50-100	11	0.11	0.001	2.3	0.001	-0.6	NS
50-500	9	0.16	0.001	3.0	0.02	-0.4	NS
100-500	10	0.07	0.001	1.8	0.002	0.0	NS

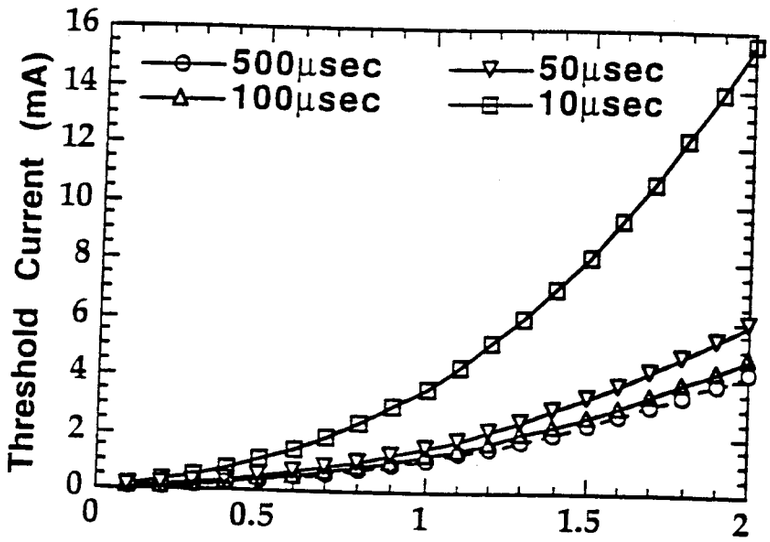

Figure 1

"THE EFFECT OF STIMULUS PULSE DURATION
ON SELECTIVITY OF NEURAL STIMULATION"
Warren M. Grill and J. Thomas Mortimer

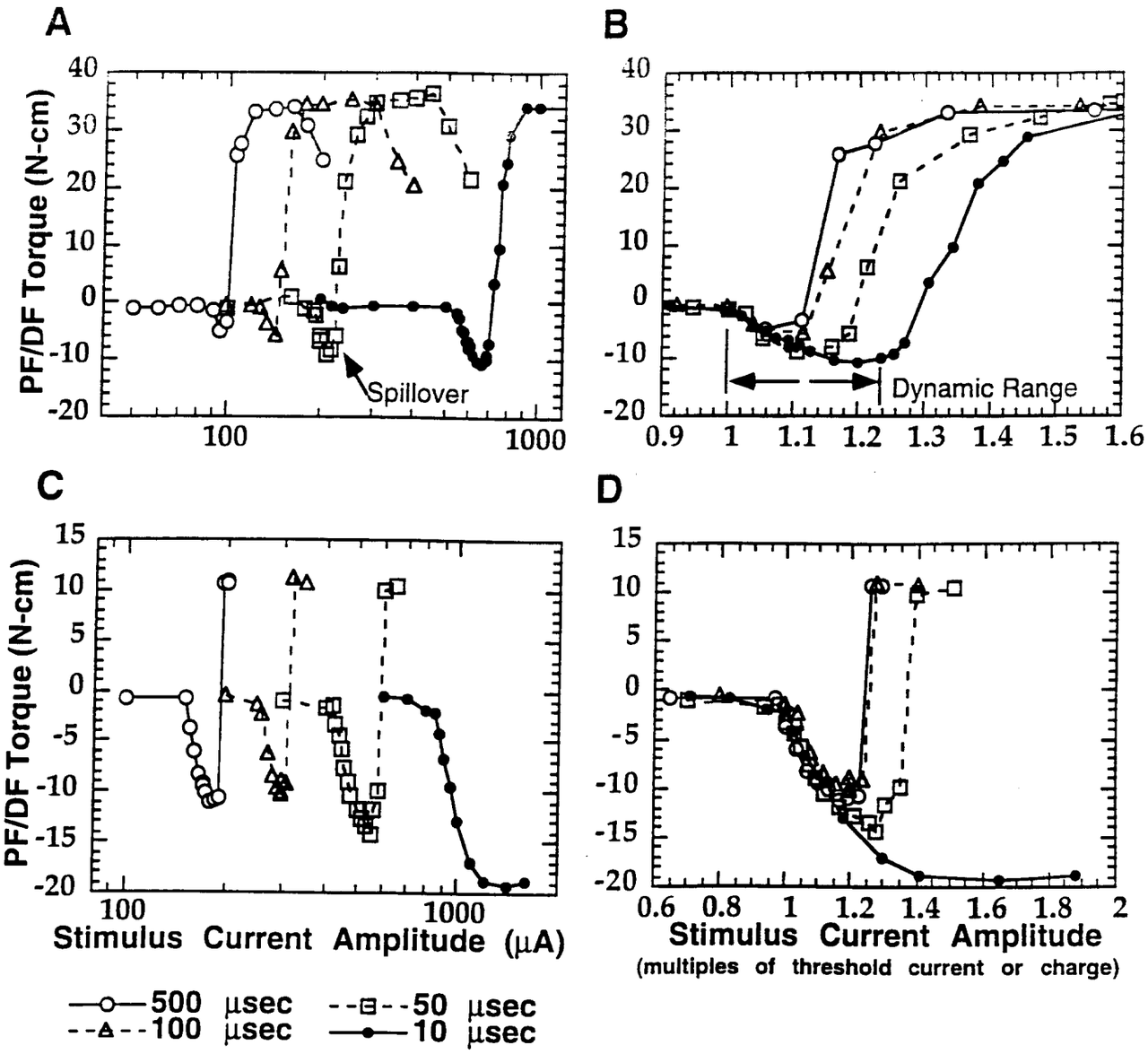

Figure 2

"THE EFFECT OF STIMULUS PULSE DURATION
ON SELECTIVITY OF NEURAL STIMULATION"
Warren M. Grill and J. Thomas Mortimer

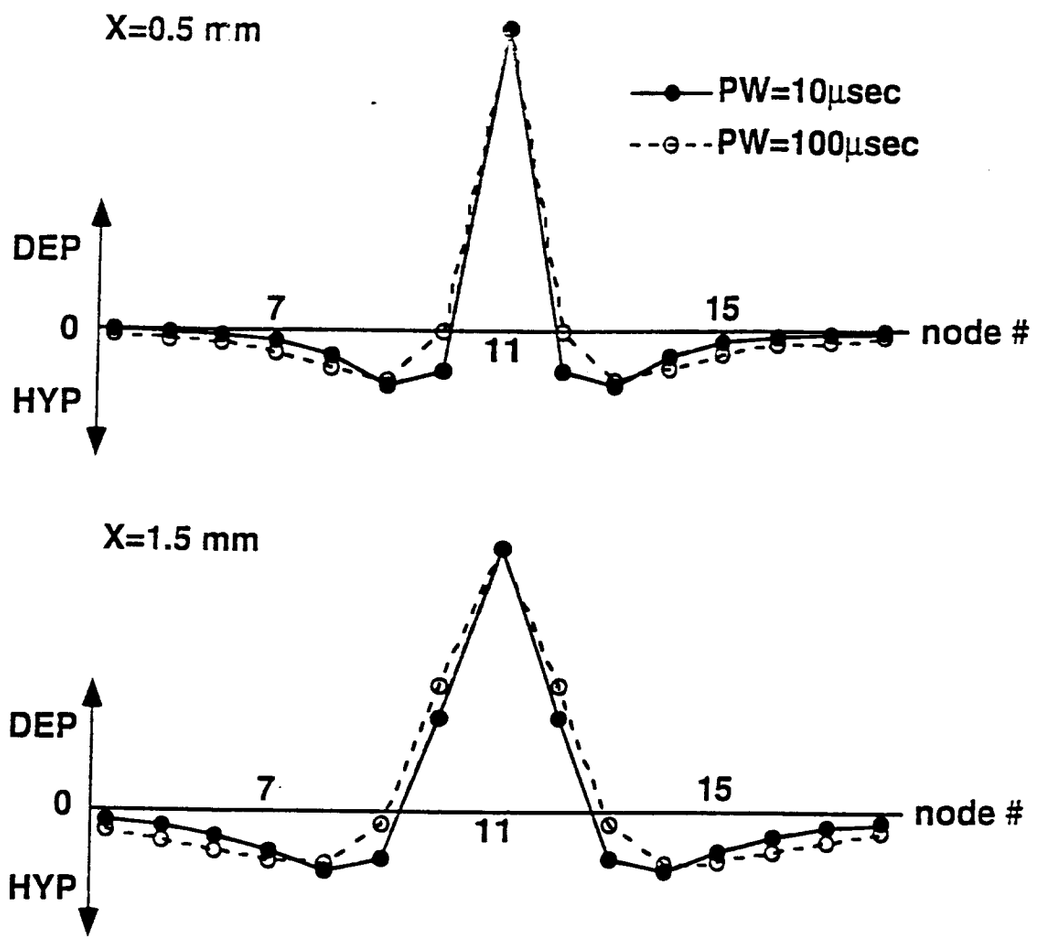

Figure 3

"THE EFFECT OF STIMULUS PULSE DURATION
ON SELECTIVITY OF NEURAL STIMULATION"
Warren M. Grill and J. Thomas Mortimer

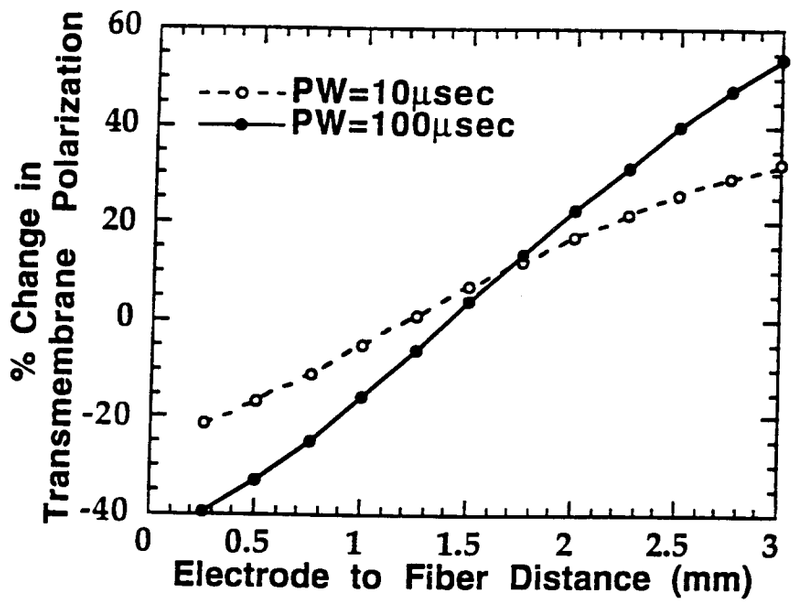

Figure 4

"THE EFFECT OF STIMULUS PULSE DURATION
ON SELECTIVITY OF NEURAL STIMULATION"
Warren M. Grill and J. Thomas Mortimer